Computer Modeling in Engineering & Sciences

Tech Science Press

https://doi.org/10.32604/cmes.2026.083259

ARTICLE

Incorporating Confidence of Evidence in Diabetes Diagnosis Using Disc T-Spherical Fuzzy Sets with AHP–TOPSIS Framework

Wafa Alagal[1,*] **and Zanyar A. Ameen**[2,*]

[1]Department of Mathematics and Statistics, College of Science, University of Jeddah, Jeddah, Saudi Arabia
[2]Department of Mathematics, College of Science, University of Duhok, Duhok, Iraq

*Corresponding Authors: Wafa Alagal. Email: waalagal@uj.edu.sa; Zanyar A. Ameen. Email: zanyar.ameen@uod.ac

Received: 31 March 2026; Accepted: 14 May 2026; Published: 30 June 2026

ABSTRACT: Diabetes remains a major global health challenge and requires diagnostic systems capable of handling uncertainty and sometimes conflicting clinical evidence. In this study, a Disc T-Spherical Fuzzy (DT-SF) TOPSIS framework is proposed for diabetes risk assessment, where the radius parameter is used to encode the confidence associated with each diagnostic attribute. The methodology also integrates the Analytic Hierarchy Process (AHP) to determine the relative importance of several key risk factors, including blood glucose, body mass index, family history, lifestyle factors, and clinical symptoms. One important feature of the proposed approach is the ternary classification scheme, which categorizes patients as Non-diabetic (N), Prediabetic (P), or Diabetic (D). In particular, this scheme allows the explicit identification of patients located in a grey zone (Class P), where early monitoring and preventive intervention may be beneficial. The proposed framework is evaluated using the Pima Indians Diabetes Dataset (PIDD). The obtained results show that the ternary DT-SF TOPSIS model achieves 89.14% accuracy, while the conventional binary thresholding method reaches 75.91%. Further analysis of the Closeness Coefficient (CC) distributions, together with threshold sensitivity examination, supports the robustness and interpretability of the proposed framework. Overall, the findings indicate that the DT-SF TOPSIS model provides a practical, confidence-weighted, and uncertainty-aware tool for multi-criteria diabetes risk assessment, with possible applications to other chronic diseases.

KEYWORDS: Spherical fuzzy sets; circular T-spherical fuzzy sets; disc T-spherical fuzzy sets; TOPSIS; diabetes diagnosis

1 Introduction

Diabetes Mellitus (DM) is a chronic metabolic condition marked by high blood glucose levels, resulting from reduced insulin secretion or insulin resistance [1]. The disease is traditionally classified into three primary clinical types: Type 1 (T1D), Type 2 (T2D), and gestational diabetes [2,3]. The incidence of diabetes in the world over the past few decades has been on the rise regardless of age. It was estimated that by 2035 there would be 592 million diabetic people [4], but the recent statistics indicate that the number will be over 642 million by 2040 [5], and around 852.5 million by 2050, according to the [2] prediction. The growth is also marked by a high financial cost; global health spending on diabetes goes above USD 1.015 trillion in 2024, which is a rise of 338 percent since 2007 [2].

Effective management of diabetes requires a sophisticated continuous care model that integrates blood glucose monitoring, dietary regulation, and physical activity [6]. However, the diagnostic process for

general practitioners is frequently complicated by the heterogeneous nature of patient symptoms and the vast array of available therapeutic interventions. With over 30 approved medications across nine distinct categories, selecting the optimal treatment path has evolved into a high-stakes, multi-objective healthcare challenge [7,8]. This complexity often leads to clinical confusion, as practitioners must balance efficacy, safety, cost, and patient self-management capabilities under conditions of significant uncertainty [9,10].

In this complex clinical environment, medical decision support systems (MDSS) have become essential tools for integrating organized clinical knowledge with patient-specific data [11]. Given that diagnostic and treatment selection involves weighing conflicting benefits and drawbacks, Multi-Criteria Decision-Making (MCDM)—a subdiscipline of operations research—offers a rigorous quantitative framework for these challenges [12,13].

However, traditional MCDM models typically rely on crisp data, which do not capture the hesitation and uncertainty often present in clinical measurements. To solve this problem, we need a better way to handle unclear or uncertain cases in diagnosis. So, this study presents a new method called the Disc T-Spherical Fuzzy (DT-SF) TOPSIS. This method helps rank the risk of diabetes in a way that is interpretable and analytically transparent. Instead of just saying "yes" or "no" for diabetes, this new model offers three possible outcomes, giving a more detailed and helpful result.

1.1 MCDM in Diabetes

In recent twenty years, MCDM methods were applied more intensively to the research in the field of diabetes since it concerns multiple factors in making the decision in diabetes and diabetes-related problems. Recently, a systematic review determined six key areas of MCDM techniques' applications in diabetes: medication choice, diagnosis, meal recommendation, management plans, evaluation of complications, and prevalence determination estimation [14].

One of the significant applications of MCDM is the choice of diabetes drugs. Having close to 30 approved drugs that fall under nine therapeutic categories, physicians have to strike a balance well between efficacy, safety, side effects, cost and patient preferences. The application of structured comparisons has been demonstrated to assist clinicians in making more evidence-based prescription decisions through several studies employing different methods, including the Analytic Hierarchy Process (AHP), fuzzy AHP, and TOPSIS, among others, as research tools [15–17]. Fuzzy versions of AHP have been particularly to solve the ambiguity that frequently occurs in expert decisions in ranking oral antidiabetic agents.

Another important area of application of MCDM is diagnosis. The high number of symptoms and overlapping risk factors of diabetes often pose a problem to general practitioners. The AHP and TOPSIS methods, which may be used together with the fuzzy logic, have been used to scale the criteria like obesity, family history, blood glucose and blood pressure [9,18]. Moreover, hybrid methods to combine MCDM with machine learning are created, which provide better forecasting results and semantics of the results obtained in forecasting challenges [19]. These methods show that using MCDM can help diagnose diabetes accurately and without delay.

MCDM methods have also been useful in dietary planning. Diabetic patients have to make daily choices between the nutritional value, glycemic index, and their personal preferences. Other techniques such as PROMETHEE and fuzzy TOPSIS have been used to provide a suggestion on the best meals to be eaten, taking into account clinical and cultural aspects [20]. In the same way, MCDM has been applied in assessing more expansive management practices, such as the use of self-management technology such as insulin pumps, mobile apps, and continuous glucose monitoring devices [10]. All these research studies emphasize the importance of MCDM to patient-centered care and technology adoption.

In addition to the management and lifestyle, MCDM was also used to evaluate the risks of diabetes complications, including neuropathy, retinopathy, and heart diseases. Clinical indicators and lifestyle factors have been combined with treatment adherence as the components of the comprehensive risk assessments with the help of approaches such as fuzzy PROMETHEE and the use of entropies to weight the components in accordance with their importance to prognosis and prognosis of therapy adherence, etc. A less prominent yet also interesting group of studies has used MCDM to approximate the prevalence of diabetes in a given population, as it entails the integration of demographic, clinical, and lifestyle variables to give more detailed projections [6]. Recently, the most favorable choice of diagnostic methodological tools has been studied as well [21]. As an example, the research involving complex bipolar fuzzy dynamic aggregation operators used an MCDM model of ranking the existing diagnostic tests capable of diagnosing diabetes mellitus identifying the Hemoglobin A1c (HbA1c) test as the most applicable among the reviewed options. This work highlights how using more advanced fuzzy logic tools can help clinicians compare different diagnostic methods, which supports the decisions they make for each patient.

In these respective applications, AHP and TOPSIS can be seen as by far the most frequently employed methods, and frequently they are further augmented with fuzzy logic to more closely model uncertainty. Fuzzy AHP has been especially effective in capturing ambiguity and hesitation in expert judgments, and fuzzy TOPSIS gives the reliable ranking in cases when the data available to it are inaccurate. However, the majority of the current research is based primarily on the classical fuzzy sets or intuitionistic fuzzy sets with the more advanced extensions of Pythagorean, spherical, and T-spherical fuzzy sets being less represented. This scenario suggests that there is demand to have models that can model uncertainty in a more rich and flexible manner.

In this respect, Disc T-Spherical Fuzzy Sets (DT-SFSs) are even more flexible and are capable of modeling membership, non-membership, and neutrality with generalized constraints along with a radius parameter, which indicates the level of confidence. Adding DT-SFSs to the classic MCDM methods like AHP and TOPSIS creates a novel framework, which is called DT–SFS TOPSIS to implement diabetes diagnosis. It is a more sophisticated system of categorizing the patients as non-diabetic, prediabetic, and diabetic.

1.2 Extended Fuzzy Sets

The development of the fuzzy set theory can be viewed as an ongoing attempt to theorize the vagueness, hesitation and uncertainty of real-life decision-making. This was pioneered by Zadeh who introduced Fuzzy Sets (FSs), in which the degree of membership (μ) of an element is given as a real number in the range $[0, 1]$. Although it was foundational, FSs were still not sufficient to describe the complexity of conflicting clinical data; Intuitionistic Fuzzy Sets (IFSs), introduced by Atanassov [22], were the first to include both (μ) and non-membership degree (ν). As the requirements for information encoding grew, the limitations of IFSs—particularly when the sum of μ and ν exceeds unity—necessitated further generalizations. Yager [23] introduced the q-Rung Orthopair Fuzzy Sets (q-ROFSs) [24], which allowed for more flexible power constraints.

Despite these progresses, many early models neglected the “neutral” degree of information, which is vital in clinical diagnostic processes. Cuong and Kreinovich [25] addressed this by introducing Picture Fuzzy Sets (PFSs), integrating a neutral membership degree (γ). To overcome the rigid linear constraints of PFSs, Mahmood et al. [26] proposed Spherical Fuzzy Sets (SFSs), and subsequently, T-Spherical Fuzzy Sets (T-SFSs) [26,27], which allowed for greater flexibility in assigning values within $[0, 1]$ via an integer exponent n.

Circular Spherical Fuzzy Set (CSFS) [28] is an important improvement to the fuzzy set theory, which aims to add a fixed radius (r) to the standard spherical fuzzy model. The model is a straight forward

generalization of the Circular Pythagorean Fuzzy Set (C-PyFS) [29]. It is based on this that the Disc Spherical Fuzzy Set (DSFS) was proposed in [28] that further develops the model by giving each particular element a specific radius (r) as opposed to a fix one. The DSFS is a natural generalization of the Disc Pythagorean Fuzzy Set (D-PyFS) [29]. In order to handle even more complicated decision settings by enlarging the squared sum constraint to $n \geq 1$ power parameter, the Disc T-Spherical Fuzzy Set (DT-SFS) has been proposed in recent literature [30]. The model is an expansion of the DSFS, which gives it a larger membership space capable of representing high-degree uncertainty. This structure establishes the mathematical basis of our proposed DT-SF TOPSIS methodology so we can encode clinical evidence, blood glucose or body mass index, with the exact level of confidence necessary to obtain an accurate diagnosis stratification.

1.3 Research Gap

In spite of the application of fuzzy MCDM techniques such as fuzzy TOPSIS and fuzzy AHP in diabetes-related decision-making problems [14], their use in diagnostic contexts remains limited. Recent studies have increasingly focused on fuzzy machine learning and deep learning models, including Adaptive Neuro-Fuzzy Inference Systems (ANFIS) [31], fuzzy convolutional neural networks (FCNN) [32], type-2 fuzzy neural networks (T2FNN) [33], and hybrid meta-heuristic fuzzy classifiers such as Genetic Fuzzy Classifiers [34] and PSO-based fuzzy classifiers [35]. Although these approaches generally achieve high predictive performance, they operate as black-box models and do not provide transparent multi-criteria reasoning suitable for clinical decision support. Moreover, existing fuzzy extension frameworks such as IFS, PyFS, SFS, T-SFS, D-SFS, and their variants have received very limited attention in diabetes diagnosis. In particular, there is almost no reported work on fuzzy MCDM approaches based on these fuzzy extension sets for diabetes diagnosis using PIDD. This reveals a clear gap in developing interpretable, uncertainty-aware decision-making frameworks that can simultaneously handle medical uncertainty and provide structured reasoning for clinical diagnosis.

1.4 Novelty and Contributions

This study is motivated by the need to develop interpretable and reliable decision-support systems for diabetes diagnosis using the PIMA Indians Diabetes Dataset (PIDD). In this context, diagnostic decision-making is challenged by uncertainty in clinical measurements and the presence of borderline cases, which cannot be adequately handled by conventional binary classification models. Although machine learning and deep learning approaches often achieve high predictive accuracy, they typically operate as black-box models and lack transparent reasoning structures required in medical decision-making.

To address these limitations, this study proposes a Disc T-spherical fuzzy TOPSIS (DT-SF TOPSIS) framework based on existing DT-Spherical Fuzzy Sets (DT-SFSs). The main contribution lies in extending the classical TOPSIS method within the DT-SFS environment, enabling the simultaneous incorporation of membership, non-membership, indeterminacy, and reliability information in the distance computation from ideal solutions. In contrast to conventional fuzzy MCDM approaches that treat all criteria information uniformly, the proposed framework explicitly integrates reliability into the ranking process, resulting in a more robust and discriminative diagnostic mechanism.

Furthermore, a structured three-way decision strategy is introduced to explicitly identify a clinical "grey zone", allowing the model to distinguish borderline patients from clearly healthy and diabetic cases. This provides a more realistic representation of diagnostic uncertainty and improves clinical interpretability, particularly in early-stage or ambiguous cases where crisp classification is insufficient.

In addition, the decision-making process is supported by an Analytic Hierarchy Process (AHP)-based weighting scheme, which ensures transparent and clinically meaningful prioritization of diagnostic attributes

such as glucose level and body mass index, while also accounting for hesitation as an auxiliary uncertainty factor. This preserves interpretability throughout the entire pipeline, from criteria weighting to final ranking relative to ideal solutions.

Finally, the proposed DT-SF TOPSIS framework is empirically validated on PIDD, demonstrating that an uncertainty-aware fuzzy MCDM approach can achieve competitive diagnostic performance while maintaining interpretability. The results confirm that the proposed framework provides a balanced trade-off between accuracy, uncertainty modeling, and explainability, addressing key limitations of existing approaches in diabetes diagnosis.

1.5 Outline of the Study

The rest of the paper is structured as follows. Section 2 reviews the Disc T-Spherical Fuzzy (DT-SF) model and its mathematical foundations. Section 3 presents the materials and methods, including patient data, the fuzzification process, and the integration of AHP within the DT-SFS TOPSIS framework. Section 4 reports the obtained results, including the computation of weights, construction of the decision matrix, and an illustrative clinical decision scenario demonstrating the practical impact of the proposed model, followed by a comparative analysis with existing fuzzy and machine learning models. Section 5 discusses the findings in detail, with particular attention to interpretability and clinical relevance. Finally, Section 6 concludes the paper and highlights possible directions for future research.

2 Disc T-Spherical Fuzzy Model [30]

Let $\mathcal{U}$ be a universal set. A Disc T-Spherical Fuzzy Set (DT-SFS) over $\mathcal{U}$ is defined by

$$F = \{(u, \mu(u), \gamma(u), \nu(u); r(u)) : u \in \mathcal{U}\},$$

where $\mu, \gamma, \nu : \mathcal{U} \to [0,1]$ are the degree membership, neutral, non-membership functions, respectively, such that

$$(\mu(u))^n + (\gamma(u))^n + (\nu(u))^n \leq 1 \tag{1}$$

for each $u \in \mathcal{U}$ and some $n \in \mathbb{Z}^+$, and $r(u) \in [0, \sqrt{3}]$ is the radius of the circle around the point $(\mu(u), \gamma(u), \nu(u))$ in the T-spherical region $\mathcal{S}$.

For simplicity, the 4-tuple $f = (\mu, \gamma, \nu; r)$ will be called a disc T-spherical fuzzy value (DT-SFV).

Fig. 1 presents the geometrical view of T-spherical region $\mathcal{S} = \{(x, y, z) : 0 \leq x^n + y^n + z^n \leq 1\}$ with different dimensions. Fig. 2 demonstrates the geometrical view of DT-SFVs $(\mu, \gamma, \nu; r)$ in certain dimension.

In this part, we shall recall some set theoretic and algebraic operations on DT-SFVs.

Let $g_1 = (\mu_1, \gamma_1, \nu_1; r_1)$ and $g_2 = (\mu_2, \gamma_2, \nu_2; r_2)$ be two DT-SFVs over $\mathcal{U}$. The following descriptions define set theoretic operations on DT-SFVs:

1. $g_1 < g_2$ if $\mu_1 \leq \mu_2$, $\gamma_1 \leq \gamma_2$, $\nu_1 \geq \nu_2$, and $r_1 \leq r_2$.
2. $g_1 = g_2$ if $g_1 < g_2$ and $g_1 > g_2$.
3. $g_1^c = (\nu_1, \gamma_1, \mu_1; r_1)$, where g_1^c denotes the complement of g_1.
4. $g_1 \bigcup_{\max} g_2 = \big(\max(\mu_1, \mu_2), \min(\gamma_1, \gamma_2), \min(\nu_1, \nu_2); \max(r_1, r_2)\big)$.
5. $g_1 \bigcup_{\min} g_2 = \big(\max(\mu_1, \mu_2), \min(\gamma_1, \gamma_2), \min(\nu_1, \nu_2); \min(r_1, r_2)\big)$.
6. $g_1 \bigcap_{\max} g_2 = \big(\min(\mu_1, \mu_2), \min(\gamma_1, \gamma_2), \max(\nu_1, \nu_2); \max(r_1, r_2)\big)$.
7. $g_1 \bigcap_{\min} g_2 = \big(\min(\mu_1, \mu_2), \min(\gamma_1, \gamma_2), \max(\nu_1, \nu_2); \min(r_1, r_2)\big)$.

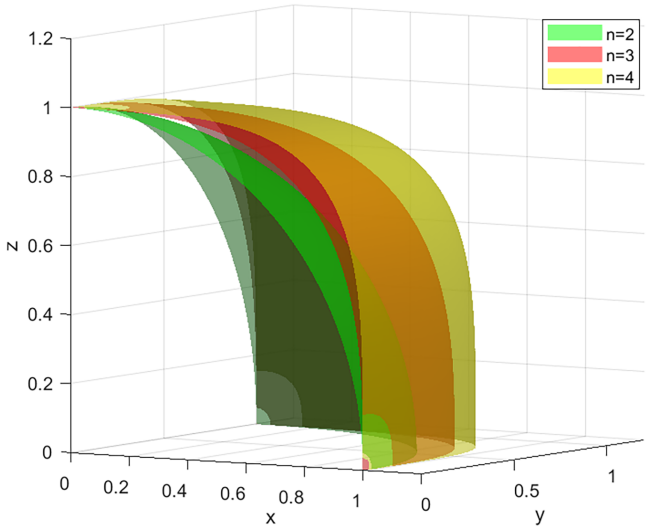

Figure 1: Geometrical representation of T-spherical region $\mathcal{S}$ for different values of n.

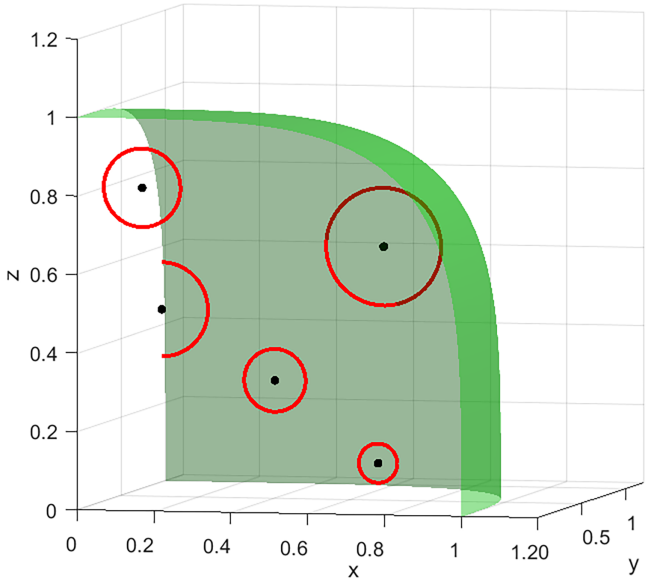

Figure 2: Geometrical representation of DT-SFVs in $\mathcal{S}$ for $n = 4$.

Let $g = (\mu, \gamma, \nu; r)$, $g_1 = (\mu_1, \gamma_1, \nu_1; r_1)$, and $g_2 = (\mu_2, \gamma_2, \nu_2; r_2)$ be DT-SFVs over $\mathcal{U}$, and $\lambda > 0$. The following descriptions define algebraic operations on DT-SFVs:

1. $g_1 \oplus_{\max} g_2 = \left(\sqrt[n]{\mu_1^n + \mu_2^n - \mu_1^n \mu_2^n}, \gamma_1\gamma_2, \nu_1\nu_2; \max(r_1, r_2)\right)$.
2. $g_1 \oplus_{\min} g_2 = \left(\sqrt[n]{\mu_1^n + \mu_2^n - \mu_1^n \mu_2^n}, \gamma_1\gamma_2, \nu_1\nu_2; \min(r_1, r_2)\right)$.
3. $g_1 \otimes_{\max} g_2 = \left(\mu_1\mu_2, \gamma_1\gamma_2, \sqrt[n]{\nu_1^n + \nu_2^n - \nu_1^n \nu_2^n}; \max(r_1, r_2)\right)$.
4. $g_1 \otimes_{\min} g_2 = \left(\mu_1\mu_2, \gamma_1\gamma_2, \sqrt[n]{\nu_1^n + \nu_2^n - \nu_1^n \nu_2^n}; \min(r_1, r_2)\right)$.
5. $\lambda g = \left(\sqrt[n]{1 - (1 - \mu^n)^\lambda}, \gamma^\lambda, \nu^\lambda, r\right)$.

6. $g^{\lambda} = \left(\mu^{\lambda}, \gamma^{\lambda}, \sqrt[n]{1-(1-\nu^{n})^{\lambda}}, r\right)$.

Score functions and distance measures are valuable decision-making tools. Score functions combine numerous criteria into a single number to rank alternatives, whereas distance measurements determine how close an option is to the optimal answer. They work together to determine the best option based on performance and proximity to the intended results.

Let $\mathcal{G} = \{g = (\mu, \gamma, \nu; r) : \mu, \gamma, \nu \in [0, 1], r \in [0, \sqrt{3}], \mu^n + \gamma^n + \nu^n \leq 1\}$ be the collection of all DT-SFVs over $\mathcal{U}$. The score function $\Phi : \mathcal{G} \to [0, 1]$ is defined by

$$\Phi(g) = \frac{1 + r + \mu^n - \gamma^n - \nu^n}{2 + \sqrt{3}}. \tag{2}$$

The accuracy function $\Psi : \mathcal{G} \to [0, 1]$ is defined by

$$\Psi(g) = \mu^n + \gamma^n + \nu^n. \tag{3}$$

Given two elements f and g of $\mathcal{G}$, we say that

- f is superior to g, denoted by $f \succ g$, if $\Phi(f) > \Phi(g)$.
- f is inferior to g, denoted by $f \prec g$, if $\Phi(f) < \Phi(g)$.
- if $\Phi(f) = \Phi(g)$, then
  - $f \succ g$ if $\Psi(f) > \Psi(g)$.
  - $f \prec g$ if $\Psi(f) < \Psi(g)$.
  - f is neutral to g, denoted by $f \simeq g$, if $\Psi(f) = \Psi(g)$.

Next, we propose the generalized distance measure as follows:

Let $g = (\mu, \gamma, \nu; r)$ and $f = (\tau, \kappa, \eta; t)$ be two DT-SFVs. The generalized distance measure d_{ω} between f and g is defined by

$$d_{\omega}(f, g) = \frac{1}{2}\left(\frac{|t - r|}{\sqrt{3}} + \frac{\sqrt[\omega]{|\tau^n - \mu^n|^{\omega} + |\kappa^n - \gamma^n|^{\omega} + |\eta^n - \nu^n|^{\omega}}}{\sqrt[\omega]{3}}\right). \tag{4}$$

If $\omega = 1$, the distance will be the Manhattan distance measure

$$d_1(f, g) = \frac{1}{2}\left(\frac{|t - r|}{\sqrt{3}} + \frac{|\tau^n - \mu^n| + |\kappa^n - \gamma^n| + |\eta^n - \nu^n|}{3}\right). \tag{5}$$

If $\omega = 2$, it will be the Euclidean distance measure

$$d_2(f, g) = \frac{1}{2}\left(\frac{|t - r| + \sqrt{(\tau^n - \mu^n)^2 + (\kappa^n - \gamma^n)^2 + (\eta^n - \nu^n)^2}}{\sqrt{3}}\right). \tag{6}$$

Theorem 1 *(Metric Properties of d_{ω}): Let $g_1 = (\mu_1, \gamma_1, \nu_1; r_1)$, $g_2 = (\mu_2, \gamma_2, \nu_2; r_2)$, and $g_3 = (\mu_3, \gamma_3, \nu_3; r_3)$ be DT-SFVs. Then, for any $\omega \geq 1$, the generalized distance d_{ω} satisfies:*

(1) $d_{\omega}(g_1, g_2) \geq 0$;
(2) $d_{\omega}(g_1, g_2) = 0$ *if and only if* $g_1 = g_2$;
(3) $d_{\omega}(g_1, g_2) = d_{\omega}(g_2, g_1)$;
(4) $d_{\omega}(g_1, g_3) \leq d_{\omega}(g_1, g_2) + d_{\omega}(g_2, g_3)$.

Proof: We prove only the triangle inequality. The remaining properties follow directly from the properties of absolute value and the fact that $t \mapsto t^{1/\omega}$ is increasing on $[0, \infty)$.

From the definition of d_ω, we have

$$d_\omega(g_i, g_j) = \frac{1}{2}\left(\frac{|r_i - r_j|}{\sqrt{3}} + \frac{\left(|\mu_i^n - \mu_j^n|^\omega + |\gamma_i^n - \gamma_j^n|^\omega + |\nu_i^n - \nu_j^n|^\omega\right)^{1/\omega}}{\sqrt[\omega]{3}} \right).$$

For the scalar component, the triangle inequality of real numbers gives

$$|r_1 - r_3| \le |r_1 - r_2| + |r_2 - r_3|.$$

For the fuzzy components, using Minkowski's inequality in $\mathbb{R}^3$ for $\omega \ge 1$, we obtain

$$\begin{aligned}(|\mu_1^n - \mu_3^n|^\omega + |\gamma_1^n - \gamma_3^n|^\omega + |\nu_1^n - \nu_3^n|^\omega)^{1/\omega} &\le (|\mu_1^n - \mu_2^n|^\omega + |\gamma_1^n - \gamma_2^n|^\omega + |\nu_1^n - \nu_2^n|^\omega)^{1/\omega} \\ &+ (|\mu_2^n - \mu_3^n|^\omega + |\gamma_2^n - \gamma_3^n|^\omega + |\nu_2^n - \nu_3^n|^\omega)^{1/\omega}.\end{aligned}$$

Dividing by $\sqrt[\omega]{3}$ and combining both scalar and fuzzy parts in the definition of d_ω yields

$$d_\omega(g_1, g_3) \le d_\omega(g_1, g_2) + d_\omega(g_2, g_3).$$

This completes the proof. □

Theorem 2 (Monotonicity Properties of d_ω): *Let* $g_1 = (\mu_1, \gamma_1, \nu_1; r_1)$, $g_2 = (\mu_2, \gamma_2, \nu_2; r_2)$, *and* $g_3 = (\mu_3, \gamma_3, \nu_3; r_3)$ *be DT-SFVs. If*

$$g_1 < g_2 < g_3,$$

then, for any $\omega \ge 1$, *the generalized distance measure* d_ω *satisfies*

$$d_\omega(g_1, g_2) \le d_\omega(g_1, g_3) \text{ and } d_\omega(g_2, g_3) \le d_\omega(g_1, g_3).$$

Proof: Since $r_1 \le r_2 \le r_3$, we have

$$|r_2 - r_1| \le |r_3 - r_1|, \qquad |r_3 - r_2| \le |r_3 - r_1|.$$

Because $x \mapsto x^n$ is increasing on $[0,1]$, it follows that

$$\mu_1^n \le \mu_2^n \le \mu_3^n, \quad \gamma_1^n \le \gamma_2^n \le \gamma_3^n, \quad \nu_1^n \ge \nu_2^n \ge \nu_3^n.$$

Hence,

$$|\mu_2^n - \mu_1^n| \le |\mu_3^n - \mu_1^n|, \quad |\gamma_2^n - \gamma_1^n| \le |\gamma_3^n - \gamma_1^n|, \quad |\nu_1^n - \nu_2^n| \le |\nu_1^n - \nu_3^n|.$$

Raising both sides of each inequality to the power $\omega \ge 1$ preserves the order:

$$\begin{aligned}&|\mu_2^n - \mu_1^n|^\omega \le |\mu_3^n - \mu_1^n|^\omega, \\ &|\gamma_2^n - \gamma_1^n|^\omega \le |\gamma_3^n - \gamma_1^n|^\omega, \\ &|\nu_1^n - \nu_2^n|^\omega \le |\nu_1^n - \nu_3^n|^\omega.\end{aligned}$$

Adding these three inequalities yields

$$|\mu_2^n - \mu_1^n|^\omega + |\gamma_2^n - \gamma_1^n|^\omega + |\nu_1^n - \nu_2^n|^\omega \le |\mu_3^n - \mu_1^n|^\omega + |\gamma_3^n - \gamma_1^n|^\omega + |\nu_1^n - \nu_3^n|^\omega.$$

Taking the ω-th root (which is monotone increasing on $[0, \infty)$) gives

$$\left(|\mu_2^n - \mu_1^n|^\omega + |\gamma_2^n - \gamma_1^n|^\omega + |\nu_1^n - \nu_2^n|^\omega\right)^{1/\omega} \le \left(|\mu_3^n - \mu_1^n|^\omega + |\gamma_3^n - \gamma_1^n|^\omega + |\nu_1^n - \nu_3^n|^\omega\right)^{1/\omega}.$$

Similarly,

$$\left(|\mu_3^n - \mu_2^n|^\omega + |\gamma_3^n - \gamma_2^n|^\omega + |\nu_2^n - \nu_3^n|^\omega\right)^{1/\omega} \le \left(|\mu_3^n - \mu_1^n|^\omega + |\gamma_3^n - \gamma_1^n|^\omega + |\nu_1^n - \nu_3^n|^\omega\right)^{1/\omega}.$$

Combining these estimates with the scalar inequalities and the definition of d_ω, we obtain

$$d_\omega(g_1, g_2) \le d_\omega(g_1, g_3), \qquad d_\omega(g_2, g_3) \le d_\omega(g_1, g_3),$$

which completes the proof. □

3 Materials and Methods

This study proposes a hybrid MCDM method for a comprehensive diabetes screening assessment, designed to classify patient health status for three distinct categories: Non-diabetic (N), Prediabetic (P), and Diabetic (D). The methodology integrates the Analytical Hierarchy Process (AHP) for criterion weighting and the Technique for Order of Preference by Similarity to Ideal Solution (TOPSIS) within a novel Disc T-spherical fuzzy (DT-SF) environment. The workflow of the proposed study is presented in Fig. 3.

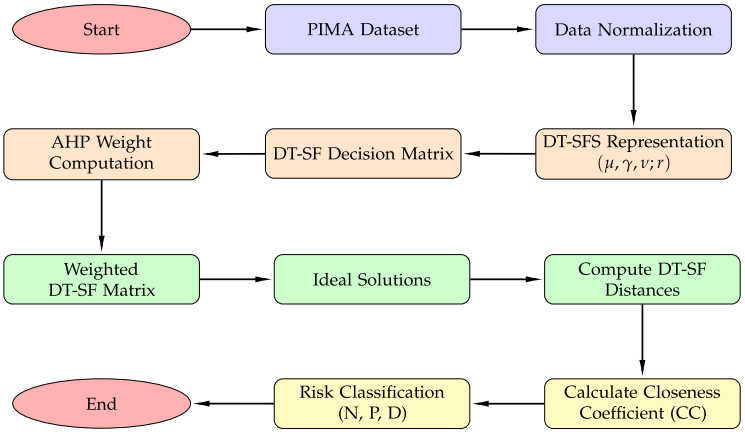

Figure 3: Flowchart of the proposed AHP–DT-SFS–TOPSIS framework for diabetes diagnosis.

3.1 Patient Data and Diagnostic Criteria

The data analysis was performed using the Pima Indians Diabetes Dataset (PIDD), which was administrated by the National Institute of Diabetes and Digestive and Kidney Diseases (NIDDK). The dataset was taken from the Kaggle website (last access: 15 December 2025) and is used as a standard benchmark to assess the performance of any predictive diagnostic models in the domain of metabolic disorders. The dataset used in this study contains clinical instances of females belonging to Pima Indian ethnicity and aged 21 or more. The class distribution in the dataset contains 268 diabetic cases (34.9%) and 500 non-diabetic cases (65.1%).

The diagnostic method covers eight independent variables that capture key physiological, anthropometric, and hereditary indicators of diabetes mellitus. These include metabolic markers such as 2-h Plasma Glucose (2hPG) concentration and Fasting Serum Insulin (FSI), alongside hemodynamic and anthropometric measures, including diastolic Blood Pressure (BP), Triceps SkinFold (TSF) thickness, and Body Mass Index (BMI), the body fat indicator based on height and weight. Furthermore, the model contains the Diabetes Pedigree Function (DPF)–a specialized metric quantifying hereditary risk based on familial history–as well as age and Gravidity (G) (number of pregnancies). The target output is a binary classification variable, where the positive class represents a diabetic diagnosis and the negative class represents a non-diabetic state. A full explanation of the diagnostic criteria, including their units and clinical meaning, is shown in Table 1.

Table 1: Diagnostic criteria for diabetes classification.

Criterion	Normal range	Unit
C_1: G	–17	Count
C_2: 2hPG	0–199	mg/dL
C_3: BP	0–122	mm Hg
C_4: TSF	0–99	mm
C_5: FSI	0–846	μU/mL
C_6: BMI	0–67.1	kg/m^2
C_7: DPF	0.0078–2.42	Score
C_8: Age	21–81	Years

3.2 Clinical Representation of DT-SFS

Medical diagnosis is rarely a matter of absolute certainty, clinical indicators often fall into "gray areas" where a patient is neither clearly healthy nor clearly ill. To capture this ambiguity, this study maps the Pima Indian clinical attributes into the DT-SF domain. This framework allows for a more granular characterization of patient health by utilizing DT-SFVs. Each clinical attribute u is represented as follows:

$$(\mu(u), \gamma(u), \nu(u); r(u)) \tag{7}$$

In this diagnostic model, the health status of a patient regarding a specific attribute is defined by four distinct parameters:

- **Membership degree (μ):** Quantifies the extent to which the clinical reading indicates a presence of diabetic risk.
- **Non-membership degree (ν):** Quantifies the extent to which the reading suggests the absence of risk.
- **Neutrality/Indeterminacy (γ):** Captures the hesitancy or middle ground, representing borderline clinical results that are inconclusive.
- **Strength of Evidence (r):** Represents the confidence level or reliability of the attribute u, where $r \in [0, \sqrt{3}]$.

To maintain the logical validity of the fuzzy space, the parameters must satisfy the power-sum constraint (1).

By incorporating the neutrality degree and the strength of evidence, the proposed system provides a more flexible and realistic decision-making environment for predicting diabetic risk compared to classical fuzzy or crisp logic approaches.

3.3 Data Normalization and Fuzzification

A special fuzzification process was applied in order to overcome the gap existing between the raw clinical values and the fuzzy decision making framework. This action brings the heterogeneous units of the PIDD into one uniform space of the form $[0,1]$ without altering the diagnostic importance of any given attribute. In line with each clinical observation u_i, we determine the membership degree of the site u_i, $\mu(u_i)$—which quantifies the presence of diabetic danger—by applying a sigmoid logistic expression:

$$\mu(u_i) = \frac{1}{1 + \exp(-k(u_i - c))} \tag{8}$$

Here, the clinical cutoff (threshold) of the attribute is given by the value c and the factor k is a scaling factor dictating the steepness of the transition point in risk. Such parameters are not arbitrary; they are adjusted according to the established medical guidelines, including the American Diabetes Association (ADA) and World Health Organization (WHO) standards. The individual values of c applied to each attribute and clinical reasons are outlined in Table 2.

Table 2: Clinical parameter justification for fuzzification.

Criterion	Cutoff (c)	Description/Reference
G	6	Total pregnancies; +5 indicates high parity and metabolic risk [36]
2hPG	140	ADA standard for 2-h blood glucose
BP	85 mmHg	Midpoint of diastolic blood pressure (80–89 mmHg)
TSF	20 mm	Median indicator of subcutaneous adiposity in the diabetic cohort [37]
FSI	166 µU/mL	Upper reference limit for 2-h postprandial serum insulin [38]
BMI	30 kg/m^2	WHO/CDC threshold for Class I Obesity
Pedigree	0.50	Threshold (≈median) based on PIDD
Age	35 years	Pivot point for increased risk of Diabetes [39]

The standard deviation (Std) σ of each of the features was chosen to define the steepness parameter k $(= 1/\sigma)$. By doing this, the sigmoid normalization is based on the natural dispersion of each of the clinical variables. With more varying features, there is a smoother transition and with less varying features, more sensitivity. This makes the normalization fair across different medical units and reduces the effect of outliers. Table 3 shows the computed Std of the data and the values of the k with each of the criteria.

Table 3: Standard deviation and steepness parameters for each criterion.

Criterion	σ	k	Description
G	3.3674	0.2970	Moderate steepness for discrete integer counts (range 0–17).
2hPG	31.9518	0.0313	Wide range (0–200+); requires a gentle curve to prevent saturation.
BP	19.3432	0.0517	Balances sensitivity across the hypertension transition zone.
TSF	15.9418	0.0627	Adjusted for high variance and potential missing data (zeros).
FSI	115.1689	0.0087	Very low k to dampen the effect of extreme outliers (up to 846).
BMI	7.879	0.1269	High sensitivity around the critical obesity threshold (30.0).
DPF	0.3311	3.0201	High amplification to distinguish tiny numeric differences (0.1 to 2.4).
Age	11.7526	0.0851	Gradual scaling to reflect metabolic changes over several decades.

The non-membership degree $v(u_i)$, representing the absence of risk, is subsequently derived as:

$$v(u_i) = 1 - \mu(u_i) \tag{9}$$

To capture the inherent uncertainty and borderline cases, the neutrality degree $\gamma(u_i)$ is calculated using the T-spherical fuzzy constraint with $n = 3$:

$$\gamma(u_i) = \sqrt[3]{1 - \mu(u_i)^3 - v(u_i)^3} \tag{10}$$

Finally, we quantify the strength of evidence r for each attribute. This parameter reflects the reliability of the diagnostic indicator, modeled as a function of the neutrality degree to ensure that higher certainty in the data results in a higher confidence score:

$$r(u_i) = \sqrt{3} \cdot (1 - \gamma(u_i)) \tag{11}$$

3.4 Criterion Weighting via Classical AHP

The Analytic Hierarchy Process (AHP), proposed by Saaty, is a widely used multi-criteria decision-making approach designed to estimate the relative significance of evaluation criteria through structured pairwise assessments. The method represents the decision problem in a hierarchical form consisting of the main objective and the associated criteria. Each pair of criteria is compared with respect to its influence on diabetes risk evaluation. In this work, expert preferences were initially expressed using linguistic importance levels, which were then translated into their equivalent numerical scores based on Saaty's standard comparison scale, as summarized in Table 4. These quantified comparisons are arranged into a reciprocal judgment matrix. The criteria weights are obtained by extracting and normalizing the principal eigenvector of this matrix so that the total weight equals one. To ensure that the judgments are logically coherent, a consistency check is performed using the consistency index and consistency ratio (CR). A CR value below 0.1 is considered acceptable, indicating that the comparisons are sufficiently consistent.

Table 4: Linguistic terms for criteria justification.

Scale	Linguistic term
1	Equal Importance
2	Weak Importance
3	Moderate Importance
4	Moderate–Strong Importance
5	Strong Importance
6	Very Strong Importance
7	Extreme Importance
8	Very Extreme Importance
9	Absolute Importance

The stepwise procedure used to compute the AHP weights is outlined in the following part:

(1) Define the set of criteria $C = \{C_k : k = 1, 2, \ldots, n\}$.

(2) Using the linguistic scale given in Table 4, construct an $n \times n$ pairwise comparison matrix M:

$$M = [m_{ij}]_{n\times n} = \begin{bmatrix} 1 & m_{12} & \cdots & m_{1n} \\ m_{21} & 1 & \cdots & m_{2n} \\ \vdots & \vdots & \ddots & \vdots \\ m_{n1} & m_{n2} & \cdots & 1 \end{bmatrix}$$

where $m_{ii} = 1$ and $m_{ji} = 1/m_{ij}$ for all i, j.

(3) Normalize the pairwise comparison matrix as follows:

$$Q = [q_{ij}]_{n\times n},$$

where each entry is computed as

$$q_{ij} = \frac{m_{ij}}{\sum_{i=1}^{n} m_{ij}}.$$

(4) The priority weight vector is computed as:

$$\boldsymbol{\lambda} = (\lambda_1, \lambda_2, \ldots, \lambda_n),$$

where

$$\lambda_i = \frac{1}{n}\sum_{j=1}^{n} q_{ij}.$$

(5) Calculate the consistency ratio CR using:

$$CR = \frac{CI}{RI}, \quad CI = \frac{\lambda_{\max} - n}{n-1}, \quad \lambda_{\max} = \frac{1}{n}\sum_{i=1}^{n} \frac{\sum_{j=1}^{n} m_{ij}\lambda_j}{\lambda_i}$$

where RI is the Random Consistency Index given Table 5. If $CR < 0.1$, the pairwise comparisons are considered consistent and the computed weights are acceptable; otherwise, the comparison matrix should be revised by an expert (go to step 2).

Table 5: *RI* values for different matrix sizes.

n	**1**	**2**	**3**	**4**	**5**	**6**	**7**	**8**	**9**	**10**
RI	0.00	0.00	0.58	0.90	1.12	1.24	1.32	1.41	1.45	1.49

3.5 DT-SF Distance-Based TOPSIS Method

The TOPSIS technique is a compromise-based MCDM method in which the most desirable alternative is determined according to its shortest distance from the positive ideal solution and farthest distance from the negative ideal solution. In the proposed framework, the evaluations are expressed by DT-SFVs, and the ranking process is performed directly through the generalized DT-SF distance measure defined in Definition 4. The procedure does not use aggregation operators and therefore preserves the DT-SFV structure during the whole computation process.

Let $A = \{A_i : i = 1, 2, \ldots, s\}$ be the set of alternatives and $C = \{C_j : j = 1, 2, \ldots, m\}$ be the set of criteria. Let $\Lambda = (\lambda_j)$ be the criteria weight vector obtained by an expert or a certain method, where $\lambda_j \geq 0$ and $\sum_{j=1}^{m} \lambda_j = 1$. Each evaluation of alternative A_i under criterion C_j is represented by a DT-SFV

$$g_{ij} = (\mu_{ij}, \gamma_{ij}, \nu_{ij}; r_{ij}),$$

satisfying constraint (1).

The DT-SF TOPSIS procedure is performed as follows:

(1) Construct the DT-SF decision matrix

$$D = (g_{ij})_{s\times m},$$

where each element g_{ij} denotes the DT-SF assessment of alternative A_i with respect to criterion C_j.

(2) According to the criterion type, obtain the normalized DT-SF matrix $H = (h_{ij})$ as follows:

- For benefit-type criteria,

$$h_{ij} = (\mu_{ij}, \gamma_{ij}, \nu_{ij}; r_{ij}).$$

- For cost-type criteria,

$$h_{ij} = (\nu_{ij}, \gamma_{ij}, \mu_{ij}; r_{ij}).$$

(3) For each criterion C_j, determine the DT-SF positive ideal solution (PIS) g_j^+ and negative ideal solution (NIS) g_j^- by

$$g_j^+ = (\mu_j^+, \gamma_j^+, \nu_j^+; r_j^+), \qquad g_j^- = (\mu_j^-, \gamma_j^-, \nu_j^-; r_j^-),$$

where

$$\mu_j^+ = \max_i \mu_{ij}, \quad \gamma_j^+ = \min_i \gamma_{ij}, \quad \nu_j^+ = \min_i \nu_{ij}, \quad r_j^+ = \max_i r_{ij},$$
$$\mu_j^- = \min_i \mu_{ij}, \quad \gamma_j^- = \max_i \gamma_{ij}, \quad \nu_j^- = \max_i \nu_{ij}, \quad r_j^- = \min_i r_{ij}.$$

(4) Using the generalized DT-SF distance $d_2(\cdot,\cdot)$ defined in Eq. (4), compute the weighted separations of each alternative A_i from the PIS and NIS as

$$D_i^+ = \sum_{j=1}^{m} \lambda_j \, d_\omega\left(h_{ij}, g_j^+\right),$$

$$D_i^- = \sum_{j=1}^{m} \lambda_j \, d_\omega\left(h_{ij}, g_j^-\right).$$

(5) For each alternative A_i, compute the relative Closeness Coefficient (CC)

$$CC_i = \frac{D_i^-}{D_i^+ + D_i^-}.$$

(6) Rank the alternatives in descending order of CC_i.

The alternative with the largest closeness coefficient is regarded as the most preferable under the DT-SF distance-based TOPSIS method.

4 Results

This section presents the numerical implementation of the hybrid AHP and DT-SF TOPSIS framework. The model was applied to the PIDD to demonstrate its ability to classify patients into three distinct categories: Non-diabetic (N), Pre-diabetic (P), and Diabetic (D). The results comprise the computed criteria weights, the patient-specific T-spherical fuzzy decision matrix, and the final classification of each patient into a three-tier diagnostic category.

4.1 Criteria Weight Computation

The initial phase involved calculating the relative importance of the eight clinical features to establish their differential impact on diabetes diagnosis. Using the AHP, a pairwise comparison matrix was constructed Table 6 to evaluate each criterion against every other based on their clinical significance. This comparison uses the standard scale from Table 4 to turn subjective judgments into measurable priorities.

Table 6: AHP pairwise comparison matrix for diabetes risk criteria.

	G	2hPG	BP	TSF	FSI	BMI	DPF	Age
G	1	1/7	1/2	1	1/3	1/5	1/5	1/5
2hPG	7	1	7	7	5	3	3	3
BP	2	1/7	1	2	1/2	1/3	1/3	1/3
TSF	1	1/7	1/2	1	1/3	1/5	1/5	1/5
FSI	3	1/5	2	3	1	1/2	1/2	1/2
BMI	5	1/3	3	5	2	1	2	1
DPF	5	1/3	3	5	2	1/2	1	1
Age	5	1/3	3	5	2	1	1	1

The final normalized weights, which give the relative significance of each clinical attribute, were then obtained using the eigenvector method. The judgment matrix was strictly tested on its consistency. The calculated Consistency Ratio (CR) was 0.0141 which is way less than the acceptable level of 0.10 and this indicates the logical consistency and trustworthiness of the pairwise comparisons.

The weights obtained and the rank of the same are shown in Table 7. This weighting is a decisive scheme because it will directly affect the following TOPSIS calculation, such that more clinically-significant factors will have a disproportionate effect on patient classification.

Table 7: Derived AHP weights for diabetes risk criteria.

Criterion	Weight
G	0.0319
2hPG	0.3526
BP	0.0518
TSF	0.0318
FSI	0.0830
BMI	0.1629
DPF	0.1384
Age	0.1476

4.2 DT-SFS Decision Matrix and Data Fuzzification

A random sample of 10 patients was randomly selected from the PIDD to assess the performance of the proposed framework. Table 8 provides the raw physiological measurements of these individuals. These values are the first crisp inputs since they demonstrate a wide variety of the clinical indicators, including the level of glucose in the body, BMI, and age, which in many cases share some overlapping features of different diagnostic categories.

Table 8: Raw clinical data for 10 randomly selected patients.

ID	G	2hPG	BP	TSF	FSI	BMI	DPF	Age
P4	1	89	66	23	94	28.1	0.167	21
P9	2	197	70	45	543	30.5	0.158	53
P17	0	118	84	47	230	45.8	0.551	31
P28	1	97	66	15	140	23.2	0.487	22
P41	3	180	64	25	70	34	0.271	26
P57	7	187	68	39	304	37.7	0.254	41
P69	1	95	66	13	38	19.6	0.334	25
P80	2	112	66	22	0	25	0.307	24
P96	6	144	72	27	228	33.9	0.255	40
P112	8	155	62	26	495	34	0.543	46

After they had presented the raw data, the values had been processed using the Section 3.3. At this stage, the crisp data points were mapped into DT-SFVs. Such conversion is necessary to represent the underlying uncertainty of medical diagnosis; instead of limiting clinical reading to a binary case, a degree of membership is given to risk presence, a degree of neutrality to ambiguity, and a degree of non-membership to risk absence.

Table 9 shows the fuzzy decision matrix that was obtained using the chosen sample. Entries are represented as DT-SFV of the form: $(\mu, \gamma, \nu; r)$. The integration of the confidence parameter r through which the parameter of confidence is put to use serves as a weight of reliability, whereby, the more precise an attribute is in its measurement or clinical significance, it serves stronger weight to the ultimate diagnosis score. Such values meet the T-spherical constraint (1), which gives a basis of TOPSIS prioritization step in the following section.

Table 9: DT-SFS decision matrix for the 10 selected patients.

Part A: First Four Criteria				
ID	**G**	**2hPG**	**BP**	**TSF**
P4	(0.1847, 0.7673, 0.8153; 0.4031)	(0.1685, 0.7491, 0.8315; 0.4346)	(0.2724, 0.8409, 0.7276; 0.2755)	(0.5469, 0.9059, 0.4531; 0.1630)
P9	(0.2336, 0.8129, 0.7664; 0.3241)	(0.8562, 0.7175, 0.1438; 0.4893)	(0.3153, 0.8652, 0.6847; 0.2335)	(0.8274, 0.7538, 0.1726; 0.4264)
P17	(0.0000, 1.0000, 0.0000; 0.0000)	(0.3343, 0.8740, 0.6657; 0.2182)	(0.4871, 0.9084, 0.5129; 0.1587)	(0.8446, 0.7329, 0.1554; 0.4625)
P28	(0.1847, 0.7673, 0.8153; 0.4031)	(0.2065, 0.7893, 0.7935; 0.3650)	(0.2724, 0.8409, 0.7276; 0.2755)	(0.4223, 0.9012, 0.5777; 0.1712)
P41	(0.2909, 0.8522, 0.7091; 0.2561)	(0.7776, 0.8035, 0.2224; 0.3403)	(0.2524, 0.8273, 0.7476; 0.2992)	(0.5777, 0.9012, 0.4223; 0.1712)
P57	(0.5737, 0.9019, 0.4263; 0.1699)	(0.8132, 0.7695, 0.1868; 0.3992)	(0.2934, 0.8536, 0.7066; 0.2536)	(0.7670, 0.8124, 0.2330; 0.3249)
P69	(0.1847, 0.7673, 0.8153; 0.4031)	(0.1965, 0.7795, 0.8035; 0.3819)	(0.2724, 0.8409, 0.7276; 0.2755)	(0.3920, 0.8942, 0.6080; 0.1832)
P80	(0.2336, 0.8129, 0.7664; 0.3241)	(0.2939, 0.8539, 0.7061; 0.2531)	(0.2724, 0.8409, 0.7276; 0.2755)	(0.5313, 0.9074, 0.4687; 0.1604)
P96	(0.5000, 0.9086, 0.5000; 0.1584)	(0.5313, 0.9074, 0.4687; 0.1604)	(0.3380, 0.8756, 0.6620; 0.2155)	(0.6080, 0.8942, 0.3920; 0.1832)
P112	(0.6443, 0.8826, 0.3557; 0.2033)	(0.6153, 0.8922, 0.3847; 0.1868)	(0.2334, 0.8127, 0.7666; 0.3244)	(0.5930, 0.8980, 0.4070; 0.1767)
Part B: Last Four Criteria				
ID	**FSI**	**BMI**	**DPF**	**Age**
P4	(0.3434, 0.8778, 0.6566; 0.2116)	(0.4400, 0.9042, 0.5600; 0.1660)	(0.2678, 0.8379, 0.7322; 0.2808)	(0.0492, 0.5198, 0.9508; 0.8318)
P9	(0.9675, 0.4553, 0.0325; 0.9434)	(0.5159, 0.9083, 0.4841; 0.1589)	(0.2625, 0.8343, 0.7375; 0.2870)	(0.0492, 0.5196, 0.9508; 0.8320)
P17	(0.6401, 0.8841, 0.3599; 0.2007)	(0.8815, 0.6793, 0.1185; 0.5555)	(0.5384, 0.9068, 0.4616; 0.1615)	(0.0508, 0.5249, 0.9492; 0.8229)
P28	(0.4418, 0.9044, 0.5582; 0.1655)	(0.2966, 0.8554, 0.7034; 0.2505)	(0.4902, 0.9084, 0.5098; 0.1586)	(0.0505, 0.5240, 0.9495; 0.8244)
P41	(0.2965, 0.8553, 0.7035; 0.2505)	(0.6243, 0.8894, 0.3757; 0.1915)	(0.3336, 0.8737, 0.666; 0.2187)	(0.0496, 0.5211, 0.9503; 0.8294)
P57	(0.7759, 0.8050, 0.2241; 0.3378)	(0.7267, 0.8415, 0.2733; 0.2746)	(0.3223, 0.8686, 0.6777; 0.2276)	(0.0496, 0.5209, 0.9504; 0.8298)
P69	(0.2401, 0.8180, 0.7599; 0.3152)	(0.2107, 0.7931, 0.7893; 0.3583)	(0.3772, 0.8899, 0.6228; 0.1907)	(0.0499, 0.5220, 0.9501; 0.8279)
P80	(0.0000, 1.0000, 0.0000; 0.0000)	(0.3464, 0.8790, 0.6536; 0.2095)	(0.3582, 0.8835, 0.6418; 0.2017)	(0.0498, 0.5216, 0.9502; 0.8285)
P96	(0.6360, 0.8856, 0.3640; 0.1982)	(0.6214, 0.8904, 0.3786; 0.1899)	(0.3230, 0.8689, 0.6770; 0.2271)	(0.0496, 0.5209, 0.9504; 0.8297)
P112	(0.9508, 0.5197, 0.0492; 0.8318)	(0.6243, 0.8894, 0.3757; 0.1915)	(0.5324, 0.9073, 0.4676; 0.1606)	(0.0507, 0.5248, 0.9493; 0.8231)

4.3 DT-SF TOPSIS and Clinical Validation

After constructing the weighted DT-SF decision matrix, the DT-SF TOPSIS procedure was applied to rank patients and derive their diagnostic priority levels. For each patient, the separation distances from the DT-SF PIS (g^+) and NIS (g^-) were computed using the proposed DT-SF distance measure. Based on these distances, the CC_i was calculated and interpreted as a unified fuzzy risk index that reflects the overall proximity of each patient profile to the diabetic risk prototype.

To improve clinical interpretability, the continuous CC_i index is mapped into a ternary diagnostic structure rather than a conventional binary decision. This multi-class mapping is consistent with the neutrality and indeterminacy components embedded in the DT-SFS representation and enables finer clinical risk stratification. The classification thresholds used in this study are summarized in Table 10.

Table 10: Classification thresholds for CC_i.

Class	Range of CC_i
Class D (Diabetic)	$CC_i < 0.42$
Class P (Prediabetic)	$0.42 \leq CC_i < 0.48$
Class N (Non-diabetic)	$CC_i \geq 0.48$

To examine threshold behavior, the relationship between classification accuracy and the closeness coefficient threshold was evaluated, with the variation of accuracy across different thresholds illustrated in Fig. 4. Building on these findings, the experimental distribution of CC scores for all 768 patients was analyzed in Fig. 5 to provide a deeper understanding of the proposed ranking measure. This distribution clearly highlights the separation pattern between the low-risk, medium-risk, and high-risk groups, providing a solid mathematical justification for the selected decision thresholds in both binary and ternary classification. Looking closer at these specific metrics on the threshold-accuracy curve, the range $0.42 \leq CC < 0.48$ was chosen as the ternary cutoff region because it corresponds to a stable plateau and aligns with the clinically established 2hPG range for prediabetes (140–199 mg/dL). Furthermore, the binary threshold $CC = 0.445$ is located at the peak of this curve, ensuring optimal separation between the diabetic and non-diabetic groups while maintaining clinical interpretability.

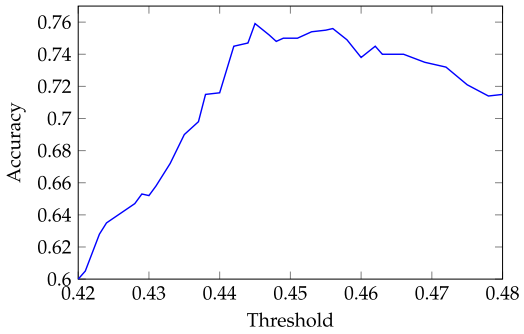

Figure 4: Impact of the CC threshold on classification accuracy.

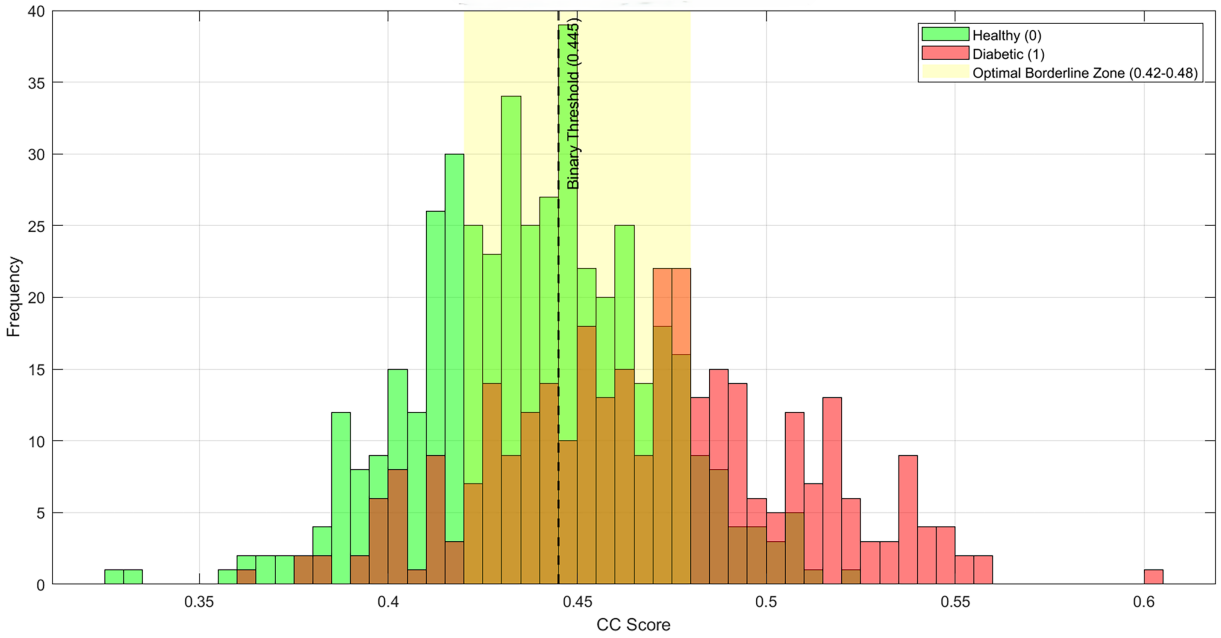

Figure 5: Distribution of CC scores for all patients. The shaded interval (0.42–0.48) corresponds to the transitional Class P (grey zone), while the binary decision threshold (CC = 0.445) lies within this region. The distribution supports the separation of low-, intermediate-, and high-risk groups.

Using the thresholds in Table 10, each patient is assigned to one of three diagnostic categories: N, P, or D. Table 11 reports the DT-SF TOPSIS classification results and compares them with the binary ground-truth labels from the PIDD.

Table 11: Comparison of DT-SF TOPSIS with PIDD ground truth.

ID	CC	Diagnosis Class	PIDD Outcome	Clinical Match
P4	0.3800	N	0	Matched
P9	0.4886	D	1	Matched
P17	0.4857	D	1	Matched
P28	0.3836	N	0	Matched
P41	0.4269	P	0*	Partial
P57	0.4821	D	1	Matched
P69	0.3549	N	0	Matched
P80	0.4027	N	0	Matched
P96	0.4468	P	0*	Partial
P112	0.4826	D	1	Matched

*Note: Class P identifies transitional risk not captured by the binary PIDD labels.

The findings indicate that in most cases, the DT-SF TOPSIS model is in agreement with the dataset ground truth. Patients who are identified to have a label of diabetic in the PIDD are always classified into Class D, whereas low-risk profiles are placed in Class N. This general consistency underlies the diagnostic consistency of the suggested DT-SF concept.

The model is sensitive to intermediate states of metabolism and this is also a strong point of the model. Class P is assigned to P41 and P96, however, the binary PIDD outcome states that they are not diabetic. Their 2-h plasma glucose data (180 and 144 mg/dL) are within the clinically given prediabetes range (140–199 mg/dL as per 2hPG requirements), which justifies the intermediate-risk designation generated by the DT-SF TOPSIS framework.

This pattern suggests that instead of depending on a single biomarker threshold, the DT-SF TOPSIS technique assesses the joint influence of several clinical features under uncertainty. Afterwards, the approach enables graded risk stratification and early-warning decision support, compared to binary classification.

Besides the illustrative subset of 10 patients, the entire dataset (768 patients) was classified and the performance of the model measured by a confusion matrix against the PIDD ground-truth labels. In this table, true negatives (TN) refers to the cases of non-diabetic identified as non-diabetic and false positive (FP) represents the non-diabetic cases which are wrongly identified as diabetic. False negatives (FN) are the cases of diabetes that are mistakenly classified as non-diabetic and the cases of diabetes that are actually diagnosed as diabetic are known as true positives (TP).

Two evaluation settings were taken into consideration. The ternary setting excluded patients in the transitional Class P (grey zone) to provide the direct and fair comparison of the binary ground-truth labels. In the binary case, classification was conducted with one threshold of closeness coefficient. The resulting confusion matrix is reported in Table 12.

Table 12: Confusion matrices for both classifications.

		Predicted Positive	**Predicted Negative**
Ternary Classification	True Positive (TP)	75	12
	False Positive (FP)	22	204
Binary Classification	True Positive (TP)	189	79
	False Positive (FP)	106	394

According to this confusion matrix, the conventional measures of diagnostic performance such as accuracy, sensitivity, specificity and F1-score were calculated. The obtained results on the ternary setting are presented in Table 13, and corresponding binary classifications are shown in Table 14.

Table 13: Performance metrics for ternary classification.

Performance metric	**Percentage**
Accuracy	89.14
Sensitivity	86.21
Specificity	90.27
F1-score	81.52

Table 14: Performance metrics for binary classification.

Performance metric	Percentage
Accuracy	75.91
Sensitivity	70.52
Specificity	78.80
F1-score	67.14

As shown in Fig. 6, the ternary classification model achieves a high performance in all evaluation measures in comparison with the binary model. Specifically, specificity and F1-score are significantly improved, which means that it is more balanced as far as sensitivity and precision are concerned.

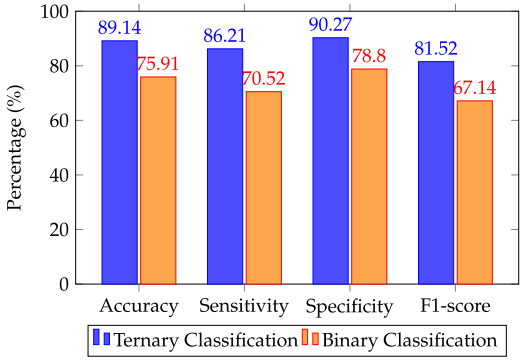

Figure 6: Performance metrics of ternary and binary classification models.

To ensure a fair and robust evaluation of the proposed DT-SF TOPSIS model, a stratified 5-fold cross-validation procedure is performed on the dataset. This approach preserves the class distribution across folds and mitigates bias associated with a single train-test split. Since the proposed framework is deterministic and does not involve a learning phase, cross-validation is used here to assess the stability and consistency of the classification results. The performance for both binary and ternary[5pc] decision settings is reported in Table 15.

Table 15: Classification performance under 5-fold cross-validation.

Fold	Binary accuracy	Ternary accuracy
1	72.08%	87.50%
2	79.87%	94.12%
3	75.97%	88.71%
4	78.43%	91.53%
5	73.20%	83.33%
Mean ± Std	75.91 ± 2.97%	89.04 ± 3.66%

These results show that the ternary framework, together with the DT-SF TOPSIS ranking, provides stronger discriminative performance when the transitional grey-zone cases are separated, while the binary thresholding scheme offers a direct comparison with conventional labeling.

To further demonstrate the practical clinical relevance of the proposed model beyond numerical validation, we present the following illustrative decision scenario.

4.4 Illustrative Clinical Decision Scenario

To demonstrate the practical clinical contribution of the proposed DT-SF TOPSIS framework, we consider representative patient cases from the PIDD dataset.

Patient No. 26 is labeled as diabetic in the binary PIMA outcome (Outcome = 1). However, the proposed model assigns this patient a CC score of 0.4374, placing them within the borderline interval (0.42–0.48), and thus classifying them as Class P (pre-diabetic/intermediate risk). From a clinical perspective, this assignment is meaningful, as the patient's glucose level (125 mg/dL) does not clearly indicate overt diabetes, suggesting a less severe or early-stage condition. In practice, this would guide the physician toward closer monitoring and lifestyle intervention rather than immediate intensive treatment.

Conversely, Patient P41 is labeled as non-diabetic in the PIMA dataset (Outcome = 0), but is assigned to Class P by the proposed model. This patient has a 2-h plasma glucose value of 180 mg/dL, which falls within the clinically recognized prediabetes range (140–199 mg/dL according to 2hPG criteria). While the binary label categorizes the patient as non-diabetic, the DT-SF TOPSIS framework identifies a clinically relevant intermediate risk. In a real-world setting, this would alert the physician to initiate preventive measures, such as dietary regulation, follow-up testing, and periodic monitoring.

These examples illustrate how the proposed model enhances clinical decision-making by refining binary classifications into a more informative risk spectrum. Rather than strictly adhering to binary labels, the DT-SF TOPSIS framework provides a nuanced interpretation that supports early detection, reduces the risk of misclassification, and enables more personalized and preventive healthcare decisions.

4.5 Comparative Analysis with Existing Models

To evaluate the relative performance of the proposed DT-SF TOPSIS framework, we compare its classification results with several representative methods reported in the literature for the PIDD dataset. A significant observation in current research is the scarcity of MCDM methodologies applied to PIDD classification. Consequently, to establish a robust benchmark, we compare our results against state-of-the-art computational intelligence techniques, including Fuzzy Machine Learning (FML), Deep Neuro-Fuzzy Systems, and Hybrid Meta-heuristic Optimization algorithms.

It is important to note that these reported results may have been obtained using different validation protocols and preprocessing pipelines; therefore, the comparison serves as a performance indicator rather than an absolute ranking. For our framework, the ternary metrics (DT-SF TOPSIS-3) are computed by focusing on the high-certainty classifications, while the binary metrics (DT-SF TOPSIS-2) utilize the optimal CC threshold of 0.445. The performance comparison is summarized in Table 16.

Table 16: Performance comparison of DT-SF TOPSIS with fuzzy reported methods on PIDD.

Reference	Year	Method	Accuracy
Vaishali et al. [34]	2017	MOEFC	78.26%
Geman et al. [31]	2017	ANFIS	84.27%
Thungrut and Wattanapongsakorn [40]	2018	FGA	87.40%
Cheruku et al. [41]	2018	RST-BOA	85.33%

(Continued)

Table 16 (continued)

Reference	Year	Method	Accuracy
Deshmukh and Fadewar [32]	2019	FCNN	95.00%
Siva Shankar and Manikandan [42]	2019	FR-GWO	81.15%
Anuradha et al. [43]	2019	ANT-FDCSM	87.70%
Lukmanto et al. [44]	2019	FSVM	89.02%
Mujawar and Jadhav [45]	2019	FES	84.00%
Raja and Pandian [35]	2020	PSO-FCM	95.42%
Aamir et al. [46]	2021	FC-1	96.47%
Aamir et al. [46]	2021	FC-2	95.38%
Chen et al. [47]	2021	CART-FIS	75.36%
Abiyev and Altiparmak [33]	2021	T2FNN (32)	87.00%
Abiyev and Altiparmak [33]	2021	T2FNN (100)	99.10%
Nagaraj and Deepalakshmi [48]	2022	IFIR-PDDM	98.87%
Alasaady et al. [49]	2022	ANFIS	92.77%
Ahmed et al. [50]	2022	FML	94.87%
Kim et al. [51]	2022	FCM-FMM	80.96%
Salem et al. [52]	2022	TFKNN	93.18%
Padrón-Tristán et al. [53]	2023	CFL	76.60%
Saleh and Hasanpour [54]	2023	FNCT	94.87%
Aris et al. [55]	2024	FR-MLJ48	97.11%
Gupta et al. [56]	2024	FPCA-SVM	82.00%
Ghabousian et al. [57]	2024	FPSO	95.47%
Arul [58]	2025	ANFIS	81.30%
Dakhare et al. [59]	2025	FL-ANN-SVM	92.14%
Kharya et al. [60]	2025	FWBARM	96.80%
Abubakar et al. [61]	2025	FES-AIA	85.00%
Noor et al. [62]	2025	FCM-ANN	81.40%
Le and Lin [63]	2025	DT2FCMAP	82.29%
Qin et al. [64]	2025	WFPRs	77.08%
This study	2026	DT-SF TOPSIS-2	75.91%
This study	2026	DT-SF TOPSIS-3	89.14%

To enhance clarity and improve the readability of the comparative results, the methods listed in Table 16 are expressed using standardized abbreviations. The detailed expansion of these abbreviations is provided in Table 17 for reference.

Table 17: Abbreviations used in Table 16.

Abbreviation	Full Model Name
MOEFC	Multi-Objective Evolutionary Fuzzy Classifier
ANFIS	Adaptive Neuro-Fuzzy Inference System
DT-NFS	Decision Tree-Based Neuro-Fuzzy System
FGA	Fuzzy Genetic Algorithm

(Continued)

Table 17 (continued)

Abbreviation	Full Model Name
RST-BOA	Rough Set Theory–Bat Optimization Algorithm
FCNN	Fuzzy Convolutional Neural Network
FR-GWO	Fuzzy Rules–Grey Wolf Optimization
ANT-FDCSM	Ant Colony-based Fuzzy Decision Classification System Model
FSVM	Fuzzy Support Vector Machine
FES	Fuzzy Expert System
PSO-FCM	Particle Swarm Optimization–Fuzzy C-Means
FC-1	Fuzzy Classifier 1
FC-2	Fuzzy Classifier 2
CART-FIS	Classification and Regression Tree Based Fuzzy Inference System
T2FNN	Type-2 Fuzzy Neural Network
IFIR-PDDM	Intelligent Fuzzy Inference Rule-based Predictive Diabetes Diagnosis Model
FML	Fused Machine Learning
FCM-FMM	Fuzzy C-Means–Fuzzy Max–Min Neural Network
TFKNN	Tuned Fuzzy K-Nearest Neighbor
CFL	Compensatory Fuzzy Logic
FNCT	Fuzzy-Neural Chaotic Tree
FR-MLJ48	Fuzzy Rules–Machine Learning J48
FPCA-SVM	Fuzzy Principal Component Analysis–Support Vector Machine
FPSO	Fuzzy Particle Swarm Optimization
PSO-ANFIS	Particle Swarm Optimization–ANFIS
FL-ANN-SVM	Fuzzy Logic–Artificial Neural Network–Support Vector Machine
FWBARM	Fuzzy Weighted Bayes Association Rule Mining
FES-AIA	Fuzzy Expert System–Atkinson Index Algorithm
FCM-ANN	Fuzzy C-Means–Artificial Neural Network
DT2FCMAP	Deep Type-2 Fuzzy Cerebellum Model Artificial Predictor
WFPRs	Weighted Fuzzy Production Rules
DT-SF TOPSIS-2	DT-SF TOPSIS Binary Diagnosis
DT-SF TOPSIS-3	DT-SF TOPSIS Ternary Diagnosis

It is important to emphasize that the accuracy values reported for the comparative methods in Table 16 are directly adopted from their respective original studies. These results may have been obtained using different experimental settings, including variations in data preprocessing, feature selection, training/testing splits, and validation strategies. Consequently, the comparison should be interpreted as a general performance reference rather than a strictly uniform or controlled evaluation. In contrast, the proposed DT-SF TOPSIS models are evaluated under a consistent framework using the PIDD, ensuring internal validity of the reported results.

These findings motivate the discussion of interpretability and robustness in the following section.

5 Discussion

The results demonstrate that the proposed DT-SF TOPSIS technique provides effective and interpretable diabetes risk classification under uncertainty. By integrating weighted clinical criteria with DT-SF representation, the model preserves uncertainty and hesitation in the data, enabling a more informative ranking and classification than traditional crisp-threshold approaches.

A key advantage of the proposed approach is the inclusion of a ternary classification scheme, which explicitly models a borderline-risk group (Class P, the grey zone). Standard PIDD labeling is binary, often merging borderline or pre-diabetic individuals into the non-diabetic class (or even to diabetic class). By isolating Class P, the ternary framework improves discriminative performance for clearly low- and high-risk groups. While the global binary accuracy was recorded at 75.91% (Sensitivity: 70.52%, Specificity: 78.80%), the ternary-aware evaluation achieved a significantly higher accuracy of 89.14% (Sensitivity: 86.21%, Specificity: 90.27%) by correctly stratifying the clinical grey zone.

An in-depth examination of the borderline interval (0.42–0.48) indicates that the model is highly sensitive. Within this range the model was able to identify 75 TPs and 204 TNs. It is worth noting that the 12 FNs were only registered in this critical zone. This small margin of error is also of clinical significance, since this will reduce chances of overlooking high-risk individuals. Moreover, the 22 FPs of Class P can be understood as Early Detections; though these patients are not considered diabetic in the PIDD ground truth, their physiological indicators indicate that they are at-risk of developing a condition that needs to be intervened early.

Fig. 5 shows the distribution of CC scores for all patients in the PIDD. Patients with CC scores between 0.42 and 0.48 fall into a grey zone, meaning they are not clearly low-risk or high-risk. This supports the idea of using a ternary decision system. Fig. 4 demonstrates how accuracy changes with different score thresholds. The best threshold (0.445) lies in a stable part of the curve. This means the model is reliable and does not change too much with small adjustments. It is important to note that the grey zone range (0.42–0.48) was not chosen randomly. It matches both the stable accuracy area from the data and the medical range for prediabetes (blood sugar levels between 140–199 mg/dL). Because the model takes into account both test results and real medical guidelines, it is easier to understand and more useful for doctors.

The results of the comparison between ternary and binary classifications show that the model enhances the categorization of borderline cases, and high performance in the majority of the patients. In addition, as demonstrated in Table 16 in earlier section, the suggested DT-SF TOPSIS model is competitive when compared to existing machine learning models such as SVM and KNN. Although direct comparison is confined to differences in validation protocols, these findings indicate that uncertainty-aware ranking based on DT-SFVs may be as accurate as conventional classifiers, and with the benefit of transparency of clinical implementation.

From a computational perspective, the proposed DT-SF TOPSIS framework remains lightweight despite its multi-stage structure. The AHP component involves a limited number of pairwise comparisons, while TOPSIS requires only vector normalization, weighting, and distance calculations. The DT-SF transformation is performed as a one-time preprocessing step without iterative learning. Therefore, the overall method is computationally efficient and suitable for practical clinical decision-support systems, where interpretability and transparency are prioritized over heavy computational cost.

At this point, it is important to note that the study has some limitations that should be considered. The model has been tested on one benchmark dataset and external validation on other clinical datasets would consolidate the research. The further work will transfer the framework to testing the various MCDM techniques and using the model with various disease databases to confirm its generalizability.

Overall, the DT-SF TOPSIS method, together with a ternary decision scheme and a grey zone, offers a useful way to assess diabetes risk. It balances satisfactory prediction accuracy and clinical understanding, especially in finding patients with early-stage risk who can be watched closely.

6 Conclusion

This paper has introduced a new diagnostic model that combines classical AHP and DT-SFS TOPSIS as the risk assessment of diabetes using the PIDD. Using the proper attributes of DT-SFSs, the model was able to effectively represent the natural uncertainty, indeterminacy, and confidence of evidence that is inherent in clinical measures—things not captured by conventional crisp or dichotomous systems of classification.

The main contribution of this study is to develop a high-resolution ternary classification scheme that outweigh the binary diagnostic approach. A mathematically based warning zone offered by the introduction of the borderline (Class P) category, which lies between the optimal range of 0.42 (minimum control) and 0.48 (maximum control), to propose a warning zone for patients who are not yet diabetics but display a substantial physiological deviation of healthy people.

The observational findings support the effectiveness of this method: the model gives a consistent binary diagnostic rate of 75.91 percent, whereas its ternary classification rate is much higher (89.14 percent). It can be argued based on this achievement that the increased resolution offered by the disc geometry enables the framework to better represent intricate clinical profiles that would otherwise be lost due to binary simplification. Notably, the capacity of the model to detect borderline cases with low false-negative rate (12 cases) indicates that the model will be an extremely sensitive and reliable clinical screening tool to fill the gap between accuracy and interpretability.

Beyond the specific case of diabetes, this framework establishes a scalable methodology for medical decision-making under uncertainty. Future work will focus on the following directions:

- Testing the DT-SFS framework on diverse real-world datasets for other chronic conditions, such as cardiovascular diseases or chronic kidney disease, to evaluate its generalizability across different clinical indicators.
- Investigating the integration of alternative MCDM methods, such as VIKOR, PROMETHEE, or WASPAS, within the DT-SF domain to compare ranking stability and diagnostic sensitivity.
- Developing adaptive thresholding techniques to account for demographic-specific variances and integrating the logic into real-time clinical decision support systems for prospective clinical deployment.

Ultimately, this framework represents a significant step toward more nuanced, interpretable, and preventative medical diagnostics, successfully balancing elite predictive performance with deep clinical insight through a white-box process.

Acknowledgement: This work was funded by the University of Jeddah, Jeddah, Saudi Arabia, under grant No. (UJ-25-DR-2048). Therefore, the authors thank the University of Jeddah for its technical and financial support. During the preparation of this work the authors used Gemini (Free Access) in some parts of this article for language editing and grammar corrections. After using this tool, the authors reviewed and edited the content as needed and takes full responsibility for the content of the publication.

Funding Statement: This research work was funded by University of Jeddah, Jeddah, Saudi Arabia, under grant number: UJ-25-DR-2048.

Author Contributions: Wafa Alagal: Conceptualization, Investigation, Formal analysis, Writing—review & editing, Funding acquisition, Project administration, Validation; Zanyar A. Ameen: Conceptualization, Formal analysis,

Writing—original draft, Writing—review & editing, Investigation, Software, Resources, Validation, Data curation, Visualization, Methodology. All authors reviewed and approved the final version of the manuscript.

Availability of Data and Materials: The dataset supporting the conclusions of this article is available in the Pima Indians Diabetes Database, hosted on Kaggle at https://www.kaggle.com/datasets/uciml/pima-indians-diabetes-database. The data was originally provided by the National Institute of Diabetes and Digestive and Kidney Diseases.

Ethics Approval: This article does not contain any studies with human participants or animals performed by the author.

Conflicts of Interest: The authors declare no conflicts of interest.

References

1. Forouhi NG, Wareham NJ. Epidemiology of diabetes. Medicine. 2010;38(11):602–6. doi:10.1016/j.mpmed.2010.08.007.
2. International Diabetes Federation. IDF diabetes atlas 2025—11th edition; 2025 [cited 2026 Mar 1]. Available from: https://diabetesatlas.org/resources/idf-diabetes-atlas-2025/.
3. Kavakiotis I, Tsave O, Salifoglou A, Maglaveras N, Vlahavas I, Chouvarda I. Machine learning and data mining methods in diabetes research. Comput Struct Biotechnol J. 2017;15:104–16. doi:10.1016/j.csbj.2016.12.005.
4. Guariguata L, Whiting DR, Hambleton I, Beagley J, Linnenkamp U, Shaw JE. Global estimates of diabetes prevalence for 2013 and projections for 2035. Diabetes Res Clin Pract. 2014;103(2):137–49. doi:10.1016/j.diabres.2013.11.002.
5. Ogurtsova K, da Rocha Fernandes JD, Huang Y, Linnenkamp U, Guariguata L, Cho NH, et al. IDF diabetes atlas: global estimates for the prevalence of diabetes for 2015 and 2040. Diabetes Res Clin Pract. 2017;128:40–50. doi:10.1016/j.diabres.2017.03.024.
6. Zulqarnain M, Dayan F, Saeed M. TOPSIS analysis for the prediction of diabetes based on general characteristics of humans. Int J Pharm Sci Res. 2018;9(7):2932–9.
7. Grant RW, Wexler DJ, Watson AJ, Lester WT, Cagliero E, Campbell EG, et al. How doctors choose medications to treat type 2 diabetes. Diabetes Care. 2007;30(6):1448–53. doi:10.2337/dc06-2499.
8. Montori VM. Selecting the right drug treatment for adults with type 2 diabetes. BMJ. 2016:i1663. doi:10.1136/bmj.i1663.
9. Abdulkareem SA, Radhi HY, Fadil YA, Mahdi H. Soft computing techniques for early diabetes prediction. Indones J Electr Eng Comput Sci. 2022;25(2):1167. doi:10.11591/ijeecs.v25.i2.pp1167-1176.
10. Contreras I, Vehi J. Artificial intelligence for diabetes management and decision support: literature review. J Med Internet Res. 2018;20(5):e10775. doi:10.2196/10775.
11. Mayo Clinic. Diabetes medication choice decision conversation aid; 2023 [cited 2023 Sep 7]. Available from: https://diabetesdecisionaid.mayoclinic.org/index.
12. Dolan JG. Multi-criteria clinical decision support: a primer on the use of multiple-criteria decision-making methods to promote evidence-based, patient-centered healthcare. Patient Patient Centered Outcomes Res. 2010;3(4):229–48. doi:10.2165/11539470-000000000-00000.
13. Peteiro-Barral D, Remeseiro B, Méndez R, Penedo MG. Evaluation of an automatic dry eye test using MCDM methods and rank correlation. Med Biol Eng Comput. 2017;55(4):527–36. doi:10.1007/s11517-016-1534-5.
14. Aldaghi T, Muzik J. Multicriteria decision-making in diabetes management and decision support: systematic review. JMIR Med Inform. 2024;12(2):e47701. doi:10.2196/47701.
15. Maruthur NM, Joy SM, Dolan JG, Shihab HM, Singh S. Use of the analytic hierarchy process for medication decision-making in type 2 diabetes. PLoS One. 2015;10(5):e0126625. doi:10.1371/journal.pone.0126625.
16. Nag K, Helal M. Multicriteria inventory classification of diabetes drugs using a comparison of AHP and fuzzy AHP models. In: Proceedings of the 2018 IEEE International Conference on Industrial Engineering and Engineering Management (IEEM); 2018 Dec 16–19; Bangkok, Thailand. p. 1456–60. doi:10.1109/IEEM.2018.8607678.

17. Chen RC, Jiang HQ, Huang CY, Bau CT. Clinical decision support system for diabetes based on ontology reasoning and TOPSIS analysis. J Healthc Eng. 2017;2017(1):4307508. doi:10.1155/2017/4307508.
18. Abbasi M, Khorasani ZM, Etminani K, Rahmanvand R. Determination of the most important risk factors of gestational diabetes in Iran by group analytical hierarchy process. Int J Reprod Biomed. 2017;15(2):109. doi:10.29252/ijrm.15.2.109.
19. Ahmed S, Roy S, Alam GR. Benchmarking and selecting optimal diabetic retinopathy detecting machine learning model using entropy and TOPSIS method. In: Proceedings of the 2021 International Conference on Electrical, Computer, Communications and Mechatronics Engineering (ICECCME); 2021 Oct 7–8; Mauritius. p. 1–6. doi:10.1109/ICECCME52200.2021.9591153.
20. Gupta K, Roy S, Poonia RC, Nayak SR, Kumar R, Alzahrani KJ, et al. Evaluating the usability of mHealth applications on type 2 diabetes mellitus using various MCDM methods. Healthcare. 2022;10(4):1–29. doi:10.3390/healthcare10010004.
21. Alolaiyan H, Liaqat M, Razaq A, Shuaib U, Baidar AW, Xin Q. Optimal selection of diagnostic method for diabetes mellitus using complex bipolar fuzzy dynamic data. Sci Rep. 2025;15(1):3921. doi:10.1038/s41598-024-84460-7.
22. Atanassov KT. Intuitionistic fuzzy sets. Fuzzy Sets Syst. 1986;20(1):87–96. doi:10.1016/s0165-0114(86)80034-3.
23. Yager RR. Pythagorean fuzzy subsets. In: Proceedings of the 2013 Joint IFSA World Congress and NAFIPS Annual Meeting (IFSA/NAFIPS); 2013 Jun 24–28; Edmonton, AB, Canada. p. 57–61. doi:10.1109/ifsa-nafips.2013.6608375.
24. Yager RR. Generalized orthopair fuzzy sets. IEEE Trans Fuzzy Syst. 2017;25(5):1222–30. doi:10.1109/tfuzz.2016.2604005.
25. Cuong BC, Kreinovich V. Picture fuzzy sets. J Comput Sci Cybern. 2014;30(4):409–20.
26. Mahmood T, Ullah K, Khan Q, Jan N. An approach toward decision-making and medical diagnosis problems using the concept of spherical fuzzy sets. Neural Comput Appl. 2019;31(11):7041–53. doi:10.1007/s00521-018-3521-2.
27. Kutlu Gündoğdu F, Kahraman C. Spherical fuzzy sets and spherical fuzzy TOPSIS method. J Intell Fuzzy Syst. 2019;36(1):337–52. doi:10.3233/jifs-181401.
28. Ashraf S. Disc spherical fuzzy sets and their application in decision making. In: Intelligent and fuzzy systems. Cham, Switzerland: Springer Nature; 2024. p. 666–74. doi:10.1007/978-3-031-70018-7_74.
29. Khan MJ, Alcantud JCR, Kumam W, Kumam P, Alreshidi NA. Expanding Pythagorean fuzzy sets with distinctive radii: disc Pythagorean fuzzy sets. Complex Intell Syst. 2023;9(6):7037–54. doi:10.1007/s40747-023-01062-y.
30. Ameen ZA, Salih HFM, Alharbi B, Asaad BA. Improving breast cancer diagnosis from imaging measurements using disc T-spherical fuzzy sets: a quantitative approach to uncertainty. Results Eng. 2026;30(1):110252. doi:10.1016/j.rineng.2026.110252.
31. Geman O, Chiuchisan I, Toderean R. Application of adaptive neuro-fuzzy inference system for diabetes classification and prediction. In: Proceedings of the 2017 E-Health and Bioengineering Conference (EHB); 2017 Jun 22–24; Sinaia, Romania. p. 639–42. doi:10.1109/ehb.2017.7995505.
32. Deshmukh T, Fadewar HS. Fuzzy deep learning for diabetes detection. In: Computing, communication and signal processing. Singapore: Springer; 2018. p. 875–82. doi:10.1007/978-981-13-1513-8_89.
33. Abiyev RH, Altiparmak H. Type-2 fuzzy neural system for diagnosis of diabetes. Math Probl Eng. 2021;2021(1):5854966. doi:10.1155/2021/5854966.
34. Vaishali R, Sasikala R, Ramasubbareddy S, Remya S, Nalluri S. Genetic algorithm based feature selection and MOE fuzzy classification algorithm on Pima Indians Diabetes dataset. In: Proceedings of the 2017 International Conference on Computing Networking and Informatics (ICCNI); 2017 Oct 29–31; Lagos, Nigeria. p. 1–5. doi:10.1109/iccni.2017.8123815.
35. Raja JB, Pandian SC. PSO-FCM based data mining model to predict diabetic disease. Comput Meth Programs Biomed. 2020;196(2):105659. doi:10.1016/j.cmpb.2020.105659.
36. Fowler-Brown AG, de Boer IH, Catov JM, Carnethon MR, Kamineni A, Kuller LH, et al. Parity and the association with diabetes in older women. Diabetes Care. 2010;33(8):1778–82. doi:10.2337/dc10-0015.
37. Sim KH, Hwang MS, Kim SY, Lee HM, Chang JY, Lee MK. The appropriateness of the length of insulin needles based on determination of skin and subcutaneous fat thickness in the abdomen and upper arm in patients with type 2 diabetes. Diabetes Metab J. 2014;38(2):120. doi:10.4093/dmj.2014.38.2.120.

38. Redcliffe Labs. Insulin PP test reports: what's the normal range and what your results mean; 2025 [cited 2026 Feb 2]. Available from: https://redcliffelabs.com/myhealth/lab-test/insulin-pp-test-reports-whats-the-normal-range-and-what-your-results-mean/.
39. Davidson KW, Barry MJ, Mangione CM, Cabana M, Caughey AB, Davis EM, et al. Screening for prediabetes and type 2 diabetes: US preventive services task force recommendation statement. JAMA. 2021;326(8):736. doi:10.1001/jama.2021.12531.
40. Thungrut W, Wattanapongsakorn N. Diabetes classification with fuzzy genetic algorithm. In: Recent advances in information and communication technology 2018. Cham, Switzerland: Springer International Publishing; 2018. p. 107–14. doi:10.1007/978-3-319-93692-5_11.
41. Cheruku R, Edla DR, Kuppili V, Dharavath R. RST-BatMiner: a fuzzy rule miner integrating rough set feature selection and Bat optimization for detection of diabetes disease. Appl Soft Comput. 2018;67(4):764–80. doi:10.1016/j.asoc.2017.06.032.
42. Siva Shankar G, Manikandan K. Diagnosis of diabetes diseases using optimized fuzzy rule set by grey wolf optimization. Pattern Recognit Lett. 2019;125:432–8. doi:10.1016/j.patrec.2019.06.005.
43. Anuradha, Singh A, Gupta G. ANT_FDCSM: a novel fuzzy rule miner derived from ant colony meta-heuristic for diagnosis of diabetic patients. J Intell Fuzzy Syst. 2019;36(1):747–60. doi:10.3233/jifs-172240.
44. Lukmanto RB, Suharjito, Nugroho A, Akbar H. Early detection of diabetes mellitus using feature selection and fuzzy support vector machine. Procedia Comput Sci. 2019;157:46–54. doi:10.1016/j.procs.2019.08.140.
45. Mujawar IK, Jadhav BT. Web-based fuzzy expert system for diabetes diagnosis. Int J Comput Sci Eng. 2019;7(2):995–1000. doi:10.26438/ijcse/v7i2.9951000.
46. Aamir KM, Sarfraz L, Ramzan M, Bilal M, Shafi J, Attique M. A fuzzy rule-based system for classification of diabetes. Sensors. 2021;21(23):8095. doi:10.3390/s21238095.
47. Chen T, Shang C, Su P, Keravnou-Papailiou E, Zhao Y, Antoniou G, et al. A decision tree-initialised neuro-fuzzy approach for clinical decision support. Artif Intell Med. 2021;111(4):101986. doi:10.1016/j.artmed.2020.101986.
48. Nagaraj P, Deepalakshmi P. An intelligent fuzzy inference rule-based expert recommendation system for predictive diabetes diagnosis. Int J Imaging Syst Tech. 2022;32(4):1373–96. doi:10.1002/ima.22710.
49. Alasaady MT, Mohd Aris TN, Sharef NM, Hamdan H. A proposed approach for diabetes diagnosis using neuro-fuzzy technique. Bulletin EEI. 2022;11(6):3590–7. doi:10.11591/eei.v11i6.4269.
50. Ahmed U, Issa GF, Khan MA, Aftab S, Khan MF, Said RAT, et al. Prediction of diabetes empowered with fused machine learning. IEEE Access. 2022;10:8529–38. doi:10.1109/access.2022.3142097.
51. Kim KB, Park HJ, Song DH. Combining supervised and unsupervised fuzzy learning algorithms for robust diabetes diagnosis. Appl Sci. 2023;13(1):351. doi:10.3390/app13010351.
52. Salem H, Shams MY, Elzeki OM, Abd Elfattah M, Al-Amri JF, Elnazer S. Fine-tuning fuzzy KNN classifier based on uncertainty membership for the medical diagnosis of diabetes. Appl Sci. 2022;12(3):950. doi:10.3390/app12030950.
53. Padrón-Tristán JF, Cruz-Reyes L, Espin-Andrade RA, Santillán CGG, Llorente-Peralta CE. Application of compensatory fuzzy logic in diabetes problem using Pima-Indians dataset. In: Hybrid intelligent systems based on extensions of fuzzy logic, neural networks and metaheuristics. Cham, Switzerland: Springer Nature; 2023. p. 199–226. doi:10.1007/978-3-031-28999-6_13.
54. Saleh B, Hasanpour H. Diabetes diagnosis from big data using fuzzy-neural chaotic tree. Trans Mach Intell. 2023;6(2):104–13. doi:10.47176/TMI.2023.104.
55. Aris T, Bakar A, Mahiddin N, Zolkepli M. Diabetes diagnosis and level of care fuzzy rule-based model utilizing supervised machine learning for classification and prediction. J Theor Appl Inf Technol. 2024;102(6):2573–86. doi:10.17762/ijritcc.v11i9.8868.
56. Gupta K, Kumar P, Upadhyaya S, Poriye M, Aggarwal S. Fuzzy logic and machine learning integration: enhancing healthcare decision-making. Int J Comput Inf Syst Ind Manag Appl. 2024;16(3):20.
57. Ghabousian R, Farhang Y, Majidzadeh K, Babazadeh Sangar A. Hybrid of particle swarm optimization algorithm and fuzzy system for diabetes diagnosis. Int J Nonlinear Anal Appl. 2024;15(2):39–46. doi:10.22075/ijnaa.2022.29575.4196.

58. Arul K. Advancing diabetes risk prediction using anfis: a fuzzy-logic approach for improved healthcare decision support. In: Proceedings of the 2025 3rd International Conference on Artificial Intelligence and Machine Learning Applications Theme: Healthcare and Internet of Things (AIMLA); 2025 Apr 29–30; Namakkal, India. p. 1–6. doi:10.1109/aimla63829.2025.11040564.
59. Dakhare BS, Mhatre SN, Jadhav N, Patil S, Patil S, Puranik J. Enhancing predictive accuracy of diabetes diagnosis employing fuzzy logic/diabetes prediction using fused machine learning. In: Intelligent computing and communication techniques. Boca Raton, FL, USA: CRC Press; 2025. p. 412–8. doi:10.1201/9781003530190-58.
60. Kharya S, Soni S, Nanda P, Urkudee G, Ojha ASS, Nayak DSK, et al. Development and validation of a novel Bayesian belief network: a reliable fuzzy weighted diabetes predictive model. Tikrit J Eng Sci. 2025;32(SP1):1–12. doi:10.25130/tjes.sp1.2025.39.
61. Abubakar U, Jibril ML, Yola AM, Usman M, Ali Jijji S. A fuzzy expert system for early diagnosis of diabetes mellitus using an atkinson index-based algorithm. Sci World J. 2025;20(2):672–80. doi:10.4314/swj.v20i2.31.
62. Noor K, Fatima U, Raees F. Meta-learning driven multi disease fuzzy neural framework for clinical risk prediction. Intell Based Med. 2025;12(7639):100315. doi:10.1016/j.ibmed.2025.100315.
63. Le CTP, Lin CM. Design of deep type-2 fuzzy cerebellum model artificial predictor for disease forecasting. Int J Fuzzy Syst. 2025;234:16812. doi:10.1007/s40815-025-02098-7.
64. Qin F, Zain AM, Zhou KQ, Zhuo DB. Hybrid weighted fuzzy production rule extraction utilizing modified harmony search and BPNN. Sci Rep. 2025;15(1):11012. doi:10.1038/s41598-025-95406-y.